ICMR 2019

8th International Conference on Multidisciplinary Research

TOF-SIMS FRAGMENT PATTERN ANALYSIS OF BORON-DOPED CHEMICAL VAPOUR DEPOSITION DIAMOND

Kim Guan Saw (a)*
*Corresponding author

(a) School of Distance Education, Universiti Sains Malaysia, 11800 Penang, Malaysia, E-mail: kgsaw@usm.my

Abstract

Chemical vapour deposition diamond has been used widely in optoelectronic applications such as sensors, detectors and electrodes. Boron doping is usually necessary for device applications to achieve *p*-type conductivity and can be done by adding various gases such as diborane (B_2H_6) or trimethyl borate ($C_3H_9BO_3$) with the methane and hydrogen gas stream into the reactor. Time-of-flight secondary ion mass spectrometry (ToF-SIMS) is a suitable technique for surface analysis of incorporated light elements in the parts-per-billion (ppb) range. However, ToF-SIMS surface analysis based on the ion fragments can be problematic due to the difficulty of obtaining reference spectra for the materials that are analysed as well as the disadvantage of detecting fragments originating from unavoidable contaminants on the sample surface. In this work, we study the fragmentation patterns of as-received boron-doped CVD diamond to identify peaks originating from the boron-doped diamond. Fragment patterns are acquired using Bi_1^+ as the primary ion source and operated in the high current bunch mode from the IONTOF instrument. Elemental carbon fragments are believed to have originated from the diamond material. As a result of boron-doping, the positive spectrum shows the presence of B^+, while the negative spectrum shows the BO^- and BO_2^- molecular fragments. The SO_3^-, $C_xH_y^-$, Cl^-, CN^-, CNO^-, $C_xH_yO_z^-$ fragments as well as $C_xH_y^+$, $C_xH_yO_z^+$, NH_4^+ and Na^+ fragments are attributed to atmospheric contaminants.

Keywords: Time-of-flight secondary ion mass spectrometry, chemical vapour deposition diamond, boron, fragment pattern analysis.

1. Introduction

Boron incorporation into the lattice of host materials is a subject of keen research (Sheng, Gao, Bao, Wang, & Xia, 2012; Tanaka & Hayashu, 2018; Kumar, Singh, Singh, & Purohit, 2011; Suzuki, Shishido, Tanaka, & Abe, 2014; Xie et al., 2013). For instance, the incorporation of boron in steel is thought to increase creep strength (Tanaka & Abe, 2014). Its location and distribution in the host lattice and the tendency to interact with other elements in the host lattice is a matter of concern as it affects the properties of the material. In recent years, boron doping in chemical vapour deposition diamond is widely used in optoelectronic and mechanical applications such as sensors, detectors and electrodes (Boussadi, Tallaire, Brinza, Pinault-Thaury, & Archard, 2018; Gracio, Fan, & Madaleno, 2010). Boron-doped CVD diamond is a *p*-type semiconducting material with electrical conductivity that depends on the doping level. At boron concentrations of less than 10^{17} cm^{-3}, conduction occurs through holes in the valence band contributed by ionised substitutional boron. However, with higher boron concentrations, conduction occurs by nearest-neighbour and variable range hopping of holes between ionised boron sites. Further increase in the doping level will result in the formation of an impurity band that gives metal-like conductivity. While the study of boron incorporation is important, it is often hampered by the difficulty of detecting this light element.

Time-of-flight secondary ion mass spectrometry (ToF-SIMS) is a highly sensitive and fast surface analysis technique that requires relatively simple preparation. It can be used to analyse many types of materials such as semiconductors, polymers, paints, metals, ceramics as well as biological samples (Wang, Jones, & Denison, 1992; Muramoto et al., 2011; Nguyen, Perander, Hyland, & Metson, 2010; Sugden & Holness, 2011). In a ToF-SIMS measurement, the material from within the top surface of the sample is analysed. Its detection limit ranges from parts-per-million (ppm) to parts-per-billion (ppb) for some species. It can distinguish ions of elements with low atomic numbers (Z < 11) as well as their isotopes with high sensitivity (Zhang et al., 2016). It is therefore a suitable technique to analyse light element dopants such as boron (Z=5) as it is more sensitive technique than x-ray photoelectron spectroscopy (XPS) or energy dispersive spectroscopy (EDS). It is difficult to detect low concentrations of boron using XPS, for instance, due to the low relative sensitivity factor.

During ToF-SIMS measurements, the sample surface is bombarded by a beam of high energy primary ions accelerated to 10 – 25 keV. The beam of primary ions ionises the molecular species originating from the sample as well as those adsorbed on the sample surface. Secondary ions that are ejected by the beam are analysed by a mass spectrometer. The depth of analysis is usually less than 1 nm in contrast to XPS that probes a depth of 1 – 10 nm. A single primary ion pulse can generate a full mass spectrum of the sample surface although its intensity is very low. Only a few secondary ions will be generated for each primary ion pulse but secondary ions of all masses are collected in parallel and the spectrum is accumulated from many primary pulses. The high sensitivity for surface species results from this ability of secondary ions of all masses to be collected in parallel together with the high transmission of the analyser and the low background due to the single ion counting. The secondary ion species that are emitted are mostly neutral, but a small percentage comes off as either a positive or a negative ion. Therefore, both positive and negative spectra can be obtained to provide information on the elemental or molecular species present on the surface of the sample. A typical spectrum consists of numerous peaks arising from the fragmentation of the molecules at the top surface, which provides a useful pattern or fingerprint. For instance, a recent study

760

(Kempson, Barnes, & Prestidge, 2016) on the therapeutic use of porous Si suggested that the presence of $SiCH_3^+$ positive ions indicates the binding of methylene blue with the Si substrate while $SiOSH_3^-$ and $SiOSCH^-$ negative ions show chemisorption via O bridging of the Si substrate and methylene blue.

However, the identification of materials based on the ion fragments can be problematic due to the difficulty of obtaining reference spectra for the materials that are analysed as well as the high sensitivity of the ToF-SIMS technique that makes it possible to detect species in the parts-per-billion (ppb) range. ToF-SIMS analysis inadvertently suffers the disadvantage of detecting fragments that originate from unavoidable contaminants on the sample surface. While in-situ ToF-SIMS measurements can be performed with almost no contaminations from the atmosphere, analysis of as-received samples in most situations faces unavoidable atmospheric contaminants, and fragmentations from these are easily detected and add to the difficulty in the identification and analysis of the molecular species from the sample. It is therefore useful to study the fragmentation patterns of as-received samples to differentiate common contaminant peaks (e.g. atmospheric aerosol particles) from peaks originating from the actual material that is being analysed. Such studies are particularly useful in the investigation of semiconductors that have been doped with low atomic concentrations of elements that act as acceptors or donors.

2. Problem Statement

Chemical vapour deposition (CVD) diamond has been used widely in optoelectronic applications such as sensors, detectors and electrodes. Boron doping is usually necessary for device applications to achieve *p*-type conductivity and can be done by adding various gases such as diborane (B_2H_6) or trimethyl borate ($C_3H_9BO_3$) with the methane and hydrogen gas stream into the reactor. The amount of boron dopant can range from parts per million (ppm) to parts per billion (ppb) depending on the type of applications and is particularly crucial in applications such as electrodes. The detection and analysis of boron in ppb can be difficult for most characterization techniques. Even XPS faces difficulty in the detection of boron in small atomic concentrations. In addition, the detection of small amounts of dopants is easily swamped by the presence of adventitious adsorbates on the CVD diamond. Analysis of the distribution of light elements such as boron with concentrations on the order of parts-per-million (ppm) to ppb is necessary for the understanding and control of the electrical and mechanical properties of the CVD diamond host material.

3. Research Questions

3.1. Will ToF-SIMS measurements using a Bi primary ion source be able to detect boron species not more than 100 ppb in CVD diamond?

3.2. What are the positive and negative ion fragments that originate from the boron dopant?

3.3. What insights can be gained into the adsorbate composition from the fragment ion patterns?

4. Purpose of the Study

In this work we analyse the fragmentation patterns of boron doped chemical vapour deposition diamond. Samples with a B concentration of not more than 10^{16} atoms/cm^3 (~ 100 ppb) were usually

categorised as lightly doped while those with a B concentration of at least 10^{19} atoms/cm^3 (~ 100 ppm) were regarded as heavily doped. While B-doped CVD diamond has been used extensively in optoelectronic and mechanical applications the detection of the incorporated B is difficult if the amount is low. Direct evidence for a low concentration of B can be problematic. Boron has a very low sensitivity in XPS measurements and a low atomic concentration in the range of ppb may not be detected. In addition, the amount of incorporated B is difficult to determine and commercial suppliers will usually provide only an approximate level of atomic concentration of B such as [B] < 0.05 ppm. The purpose of this work is to understand the fragmentation patterns from as-received B-doped CVD diamond that has been obtained commercially without details of its fabrication such as the boron source and the actual amount of B atomic concentration.

5. Research Methods

The B-doped CVD diamond used in this work has a dark brown appearance and measures 4.5 mm × 4.5 mm × 0.5 mm. The sample which was obtained through a commercial supplier has a low B concentration of not more than 10^{16} atoms/cm^3 (~ 100 ppb). Both sides of the sample were polished (Ra < 30 nm). The quality of the CVD diamond was first ascertained using micro-Raman spectroscopy before being subject to ToF-SIMS analysis. The Ar line of excitation was used (λ = 514.5 nm) for the Raman measurements at room temperature. The IONTOF IV instrument with Bi_1^+ as the primary ion source was used for the ToF-SIMS analysis. The primary ion beam is rastered over an area of 100 μm×100 μm at 25 keV. Spectral collection was subsequently obtained from an area of 100 μm×100 μm. A pulsed electron flood source was used for charge neutralization. The primary ion dose is 4.49×10^8 cm^{-2}. Both positive and negative spectra were collected in the high current bunch mode at a high mass resolution (m/Δm) of 9000 at m/z = 29. Elemental ions together with molecular fragments in the mass range m/z = 1 to 100 obtained in both positive and negative ion spectra were reported in this work.

6. Findings

The Raman measurements in Fig. 1 show a symmetrical and an intense peak at 1332.2 cm^{-1} (FWHM = 4 cm^{-1}), suggesting the CVD diamond is of good crystalline quality. It is well-known that the Raman spectrum of single crystal diamond is dominated by the first-order Raman line at 1332 cm^{-1}, which corresponds to the vibrations of the two inter-penetrating cubic sub-lattices (Prawer & Nemanich, 2004). This Raman peak arising from the diamond phonon is a symmetric Lorentzian at low boron concentrations. With heavier boron concentration above 10^{20} cm^{-3}, the peak is likely to shift to lower wavenumbers (i.e. less than 1332 cm^{-1}) and also features an asymmetric Fano-like line-shape caused by a quantum mechanical interference between the zone-centre Raman-active optical phonon and the continuum of electronic states induced by the boron impurities.

We are not able to observe any Fano effect from the Raman measurements that is usually associated with boron-doping since the amount of boron is extremely small. The Fano resonance in diamond is a resonant scattering of light where an incident photon (light) interacts with a vibrational mode of the diamond causing the photon energy to be shifted, which in principle can be detected by Raman

measurements. The absence of the Fano asymmetry feature suggests that Raman spectroscopy could not detect the small atomic concentration of boron dopants in the sample. This is not surprising as our sample is believed to have a boron concentration of less than 10^{20} cm^{-3}.
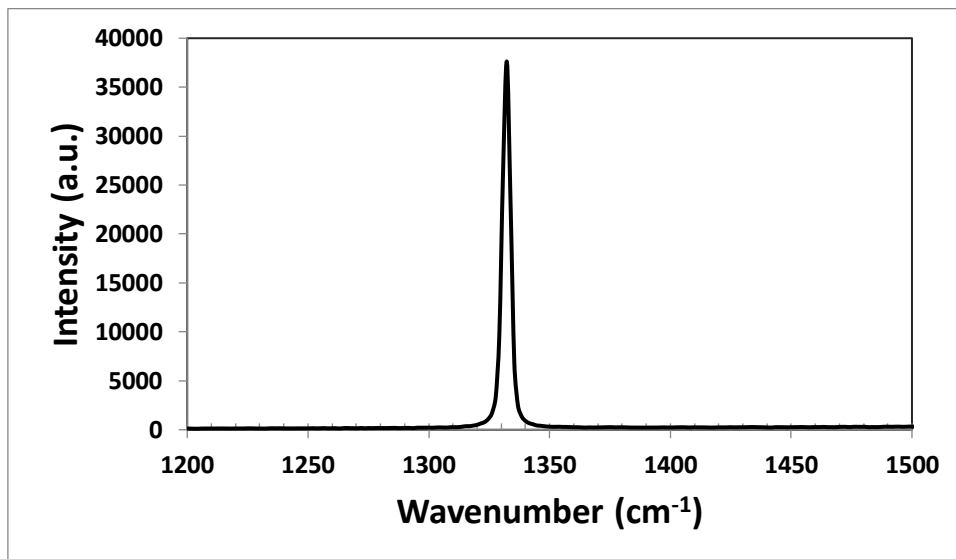

Figure 01. Raman spectrum of the B-doped CVD diamond

The symmetrical and intense peak at 1332.2 2 cm^{-1} (FWHM = 4 cm^{-1}) indicates that the CVD diamond is of good quality. The absence of the Fano asymmetry feature is probably due to the small atomic concentration of boron dopants.

In the positive spectrum (Figure 2), a B$^+$ peak and a C$^+$ peak observed at m/z = 11.0088 and m/z = 11.9995, respectively, are attributed to the boron dopant and carbon originating from the CVD diamond. Figure 3 shows the B$^+$ peak that has been isolated and magnified. The B$^+$ peak at m/z = 11.0088 is the only peak associated with boron in the positive ion spectrum. Apart from these, peaks attributed to atmospheric contaminants such as CH$_3^+$, NH$_4^+$ and Na$^+$ were seen at m/z = 15.0229, 18.0338, and 22.989, respectively.
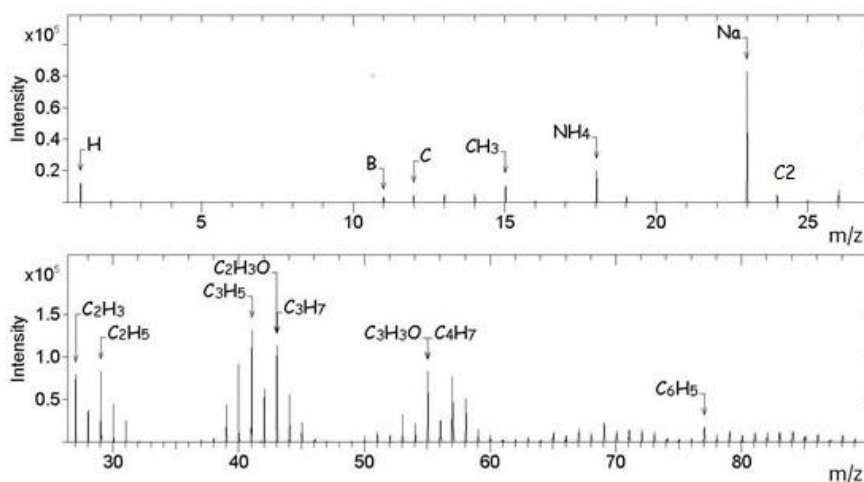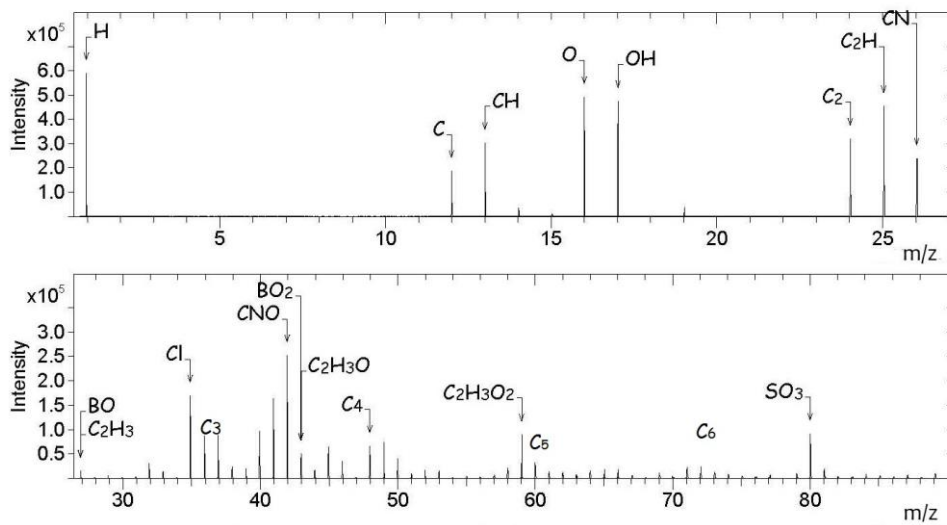

**Figure 02.** The positive ion fragment pattern for boron doped CVD diamond
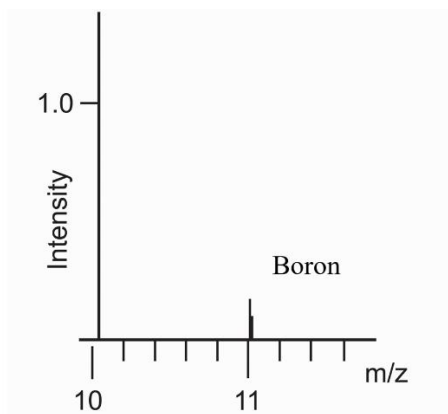
Figure 03. The B^+ peak that has been magnified. The other peaks have been omitted

In the negative ion spectrum (Figure 4), C^-, C_2^-, C_3^-, C_4^-, C_5^-, and C_6^- fragments were observed at m/z = 12, 24, 36, 48, 60 and 72, respectively. While C^- secondary ions are likely to come from carbonates and carbides, we suggest that they originate from the CVD diamond as the normalised intensity of these peaks increases in some samples where sputtering cleaning was performed. Figure 4 also shows the presence of CH^-, C_2H^-, $C_2H_3^-$ at m/z = 13, 25 and 27, respectively. While it is possible that $C_xH_y^-$ fragments may have originated from the CVD diamond due to a copious amount of hydrogen in the CVD environment during the fabrication process (Saw et al., 2003; Saw & du Plessis, 2005), we attribute them to adventitious hydrocarbons on the sample surface. The SO_3^- peak at m/z = 79.9570 as well as the Cl^-, CN^-, CNO^- and several $C_xH_yO_z$ fragments are attributed to atmospheric aerosol particles on the sample surface (Zhang et al., 2016; Zhu, Olson, & Beebe, 2001). Preliminary XPS investigations on similar as-received boron-doped CVD diamond samples show peaks belonging to S 2p and S 2s, N 1s as well as O 1s that are likely to have originated from adventitious hydrocarbons, carbonates or other atmospheric contaminants. The BO^- and BO_2^- fragment ions at m/z = 27.0048 and m/z = 42.9998, respectively, are likely to be from the source of the boron dopant. The oxygen-containing ion fragment which could have originated from trimethyl borate ($C_3H_9BO_3$) or tripropyl borate ($C_9H_{21}BO_3$) or a similar compound that was used as a source of boron for the CVD diamond. The BO^- and BO_2^- are found in the lower mass region ($m/z < 50$). These are essentially the $^{11}B^{16}O^-$ (m/z = 27.0048), and $^{11}B^{16}O_2^-$ (m/z = 42.9998) ion fragments. With high mass resolution, the BO^- and BO_2^- can be distinguished from the neighbouring peaks $C_2H_3^-$ and $C_2H^3O^-$ that are located at m/z = 27.0239 and 43.0196, respectively (Figure 5). Further investigations into the actual source of oxygen of these fragments will be done in another study.

Figure 04. The negative ion fragment pattern for boron doped CVD diamond
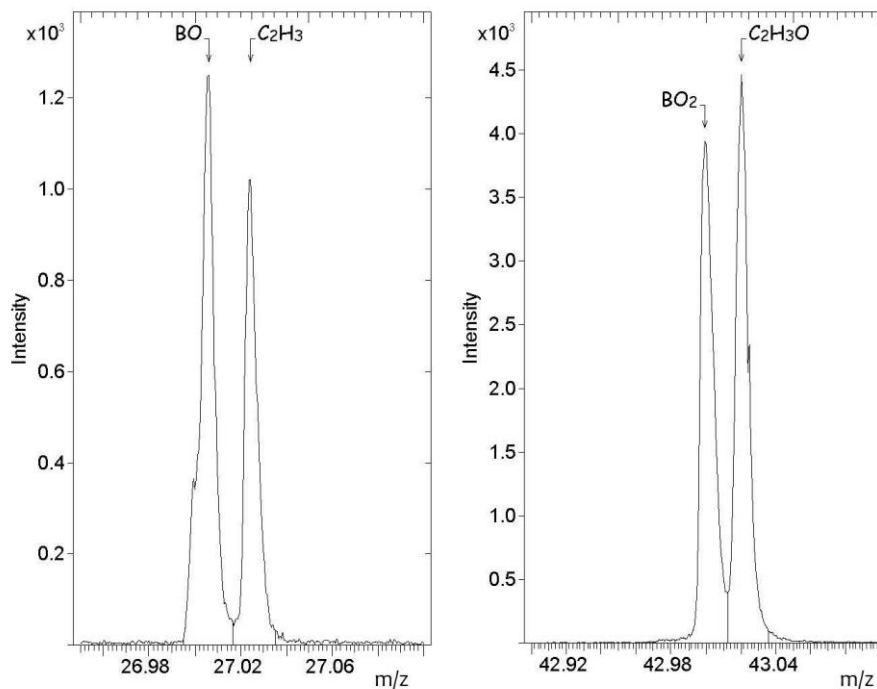
Figure 05. The BO⁻ and BO₂⁻ peaks that originate from the boron dopant can be distinguished from neighbouring peaks of C₂H₃⁻ and C₂H₃O⁻

The ToF-SIMS analysis of the as-received boron-doped CVD diamond thus shows that fragments originating from the atmospheric contaminants form a fairly large part of both the positive and negative ion spectra. This is not surprising as secondary ions such as Li^+, F^-, O^-, Na^+, Mg^+, Al^+, Si^+, NH_4^+, $C_3H_3^+$, $C_7H_7^+$, C_2H^-, NO_2^-, CN^-, CNS^-, SO_3^-, SO_2^- and HSO_4^- have been detected in atmospheric aerosol particles in recent studies (Zhang et al., 2016; Zhu et al., 2001). It should be noted that Na^+ was frequently found on the aerosol particles suggesting that sodium compounds could be present as atmospheric contaminants. There were indications that sodium compounds in the atmosphere accumulate on the surfaces of aerosol particles easily when the relative humidity is high.

7. Conclusion

It can be concluded that ToF-SIMS measurements using a Bi^+ primary ion source are able to detect boron species not more than 100 ppb in CVD diamond. Both positive and negative ion spectra show fragments that originate from the boron dopant. In the positive ion spectra only $^{11}B^+$ is observed while in the negative ion spectra the BO^- and BO_2^- are observed. Peaks from SO_3^-, $C_xH_y^-$, Cl^-, CN^-, CNO^-, $C_xH_yO_z^-$, $C_xH_y^+$, $C_xH_yO_z^+$, NH_4^+ and Na^+ are attributed to atmospheric contaminants.

Acknowledgments

References

Boussadi, A., Tallaire, A., Brinza, O., Pinault-Thaury, M. A., & Achard, J. (2018). Thick heavily boron doped CVD diamond films homoepitaxially grown on (111)-oriented substrates. *Diam. Relat. Mater.*, *79*, 108 – 111.

Gracio, J. J., Fan, Q. H., & Madaleno, J. C. (2010). Diamond growth by chemical vapour deposition. *J Phys. D: Appl. Phys, 43*(37), 374017.

Kempson, I. M., Barnes, T. J., & Prestidge, C.A. (2016). Use of TOF-SIMS to study adsorption and loading behavior of methylene blue and papain in a nano-porous silicon layer. *J. Am. Soc. Mass Spectrom., 21*, 254 –260.

Kumar, V., Singh, R. G., Singh, F., & Purohit, L. P. (2011). Highly transparent and conducting boron doped zinc oxide films for window of dye sensitized solar cell applications. *J. Alloy Compd, 544,* 120–124.

Muramoto, S., Graham, D. J., Wagner, M. S., Lee, T. G., Moon, D. W., & Castner, D. G. (2011). ToF-SIMS Analysis of Adsorbed Proteins: Principal Component Analysis of the Primary Ion Species Effect on the Protein Fragmentation Patterns. *J. Phys. Chem. C., 115,* 24247–24255.

Nguyen, C. L., Perander, L. M., Hyland, M. M., & Metson, J. B. (2010). TOF-SIMS studies of intercalated Gibbsite and Bayerite. *Surf. Interface Anal.*, *43*, 432–435.

Prawer, S., & Nemanich, R. J. (2004). Raman Spectroscopy of Diamond and Doped Diamond. *Philosophical Transactions: Mathematical, Physical and Engineering Sciences, 362*(1824), 2537–2565.

Saw, K. G., & du Plessis, J. (2005). Diamond growth on faceted sapphire and the charged cluster model. *J. Cryst. Growth, 279*(3-4), 349-356.

Saw, K. G., Andrienko, I., Cimmino, A., Spizzirri, P., Prawer, S., & du Plessis, J. (2003). Growth of diamond on α-(0 0 0 1) sapphire substrates. *Diam. Relat. Mater., 12*(10-11), 1663-1669.

Sheng, Z., Gao, H., Bao, W., Wang, F., & Xia, X. (2012). Synthesis of boron-doped graphene for oxygen reduction reaction in fuel cells. *J. Mat. Chem.*, *22*(2), 390-395.

Sugden, M., & Holness, M. (2011). Time-of-flight secondary ion mass spectrometer: a novel tool for lipid imaging. *Clin. Lipido.*, *6*(4), 437-445.

Suzuki, S., Shishido, R., Tanaka, T., & Abe, F. (2014). Characterization of the Inhomogeneous Distribution of Light Elements in Ferritic Heat-Resistant Steels by Secondary Ion Mass Spectrometry. *ISIJ International, 54*(4), 885–892.

Tanaka, T., & Hayashu, S. (2018). Analysis of the distribution of light elements in steels by Time-of-Flight Secondary Ion Mass Spectrometry (ToF-SIMS). Nippon Steel & Sumitomo Metal Technical Report No. 118.

Wang, D., Jones, F. R., & Denison, P. (1992). TOF SIMS and XPS study of the interaction of hydrolysed γ-aminopropyltriethoxysilane with E-glass surfaces. *J. Adhesion Sci. Techn.*, *6*(1), 79-98,

Xie, M., Li, D., Chen, L., Wang, F., Zhu, X., & Yang, D. (2013). The location and doping effect of boron in Si nanocrystals embedded silicon oxide film. *Appl. Phys. Lett., 102*, 123108.

Zhang, Z., Li, H., Liu, H., Ni, R., Li, J., Deng, L., …Li, W. (2016). A preliminary analysis of the surface chemistry of atmospheric aerosol particles in a typical urban area of Beijing. *J. Environ. Sci., 47*, 71-81.

Zhu, Y. J., Olson, N., & Beebe, T. P. (2001). Surface Chemical Characterization of 2.5 μm particulates (PM$_{2.5}$) from air pollution in Salt Lake City using TOF-SIMS, XPS, and FTIR. *Environ. Sci. Technol., 35*, 3113-3121.